Spectral studies of Flat Spectrum Radio Quasars: constraining models at GeV energies

Richard J G Britto[1,*], Soebur Razzaque[1] and Benoit Lott[2], on behalf of the Fermi-LAT Collaboration

[1] Department of Physics, University of Johannesburg, APK Campus, Auckland Park 2006, South Africa

[2] Centre d'Études Nucléaires de Bordeaux-Gradignan, Université Bordeaux 1, IN2P3/CNRS, 33175 Gradignan, France

E-mail: * rbritto@uj.ac.za

Abstract. Active Galactic Nuclei (AGNs) at the centres of distant galaxies are understood to be powered by the gravitational energy of supermassive black holes accreting matter from their surroundings and releasing extraordinary amounts of energy through two symmetric jets of ultrarelativistic particles and photons. Blazars are a class of AGNs with one jet directed towards us. A subclass of them are called Flat Spectrum Radio Quasars (FSRQ), which are among the brightest AGNs and have been detected up to redshift z > 3. We have analysed 5.5 years of data (2008-2014) from the Large Area Telescope (LAT) of the Fermi gamma-ray space observatory and performed spectral analysis of bright FSRQs in the 100 MeV-200 GeV energy range. Our study focuses on the spectral modification due to $\gamma\gamma$ absorption of > GeV photons interacting with Lyα, OIV and Lyβ photons in the broad line region (BLR). As the sensitivity of this analysis does not constrain the model very much, we can only rule out a very large absorption feature in the gamma-ray spectrum, indicating that the gamma ray emission region would not be located deep within the BLR.

1. Introduction

Blazars, a class of AGN, are the most luminous objects of the Universe, and release a tremendous amont of energy through a pair of jets of plasma ejected at relativistic velocities. Blazar jets produce radiation accross the whole elecromagnetic spectrum, from radio waves to γ rays. They exhibit a characteristic double-bump spectral energy distribution (SED). The dominant radiation production process is understood to be synchroton emission for the visible-UV range (first bump), whereas the X-ray/gamma-ray band (second bump) can be modeled by both leptonic and hadronic processes, although the inverse Compton process is most often used in modeling.

Flat spectrum radio quasars (FSRQs), a sub-class of blazars, are generally more luminous and at higher redshift than the BL Lacs which constitute the other subclass of blazars. A specific characteristic of FSRQs is a broad-line emission spectrum, that suggests the presence of clouds and intense radiation fields at a relatively close distance from the supermassive black hole. γ rays can be produced within the jet or/and by the interaction of the particles from the jets with visible and UV photons emitted in the broad-line region (BLR). If γ rays are produced within the BLR, it is expected that they would also undergo $\gamma\gamma \rightarrow e^{-}e^{+}$ interactions with BLR photons [10]. The radiation spectrum of the BLR would suggest that this absorption effect

could be measured in the 10-100 GeV band. The Large Area Telescope (LAT) onboard the Fermi Gamma Ray Space Observatory is sensitive to γ rays between 20 MeV and 300 GeV [3], and is the appropriate instrument for studying this effect and constraining the γ-ray emission region within the BLR by fitting Fermi-LAT spectral data. Traditionally, the BLR was modeled as a spherical thick shell-type structure while more modern models assume a flat BLR [11, 8].

We present the 5.5 yr Fermi-LAT data sample and the analysis procedure in Section 2. In Section 3 we present our modeling of the opacity $\tau_{\gamma\gamma}(E, z)$. We present our results and discussion in Section 4 and give perspectives on further studies.

2. Data sample and analysis

We selected a sample of 7 bright FSRQs from the upcoming "Third LAT AGN catalog" (3LAC): PKS 1510-089 (redshift z=0.360), 4C +21.35 (also known as PKS 1222+216, z=0.434), 3C 279 (z=0.536), 3C 454.3 (z=0.859), 4C +55.17 (z=0.899), PKS 0454-234 (z=1.003), PKS 1502+106 (z=1.839). We derived the BLR luminosity for each source, using [9, 13]. We displayed these values in units of $10^{44} erg\ s^{-1}$, in the order of the source list: 5.62, 15.80, 3.10, 33.00, 3.80, 3.70 and 17.50. For each source, we analysed about 5.5 years of data (from August 2008 up to at least January 2014). PKS 1510-089 was also studied during its Feb-Apr 2012 flare, and showed along with the data taken by MAGIC during the same period [2]. The brightest flare ever detected in gamma was seen from 3C 454.3 in Sep-Dec 2010. As flaring activity affects the shape of the SEDs, we studied this source separately during its Sep-Dec 2010 giant flare [1], during the first two years of data before the flare, and during the last 3 years of data after the flare when it was mostly quiescent.

Our data analysis was performed using the public release of the Fermi Science Tools *v9r32p5-fssc-20130916*[1] and the intrument response function *PASS7_V15_SOURCE*. For each data sample, we considered all the photons from a region of 10 degree radius around the source of interest, and we estimated the signal constribution from other sources in a 20 degrees field of view, using an unbinned likelihood algorithm (*gtlike* science tool).

3. Modeling of the opacity of the BLR

We assume a model for the BLR luminosity and radius as $L_{BLR} = 0.1 L_{Disc}$ and $R_{BLR} = 10^{17}(L_{disc}/10^{45}\, erg/s)^{0.5}$ cm, respectively, where L_{Disc} is the accretion disc luminosity [4, 6]. We also assume that BLR luminosity is dominated by Lyα and OIV+Lyβ lines with relative flux ratio 1 : 0.18 [12]. We model the Lyα and OIV+Lyβ lines as Breit-Wigner functions with peak energies $\epsilon_1 = 10.2$ eV and $\epsilon_2 = 12.04$ eV, with widths $\omega_1 = 0.8$ eV and $\omega_2 = 0.2$ eV, respectively. The $\gamma\gamma \to e^- e^+$ process has a threshold $E \approx 25.6/(1+z)$ GeV for Lyα photons, where E is the γ-ray energy.

The differential opacity per unit distance for γ rays passing through the BLR will then be written as:

$$\frac{d\tau_{\gamma\gamma}}{dx}(E,z) = \frac{r_0^2}{2}\left[\frac{m^2c^4}{E(1+z)}\right]^2 \sum_{i=1}^{2}\left(n_i\omega_i \int_{\frac{m^2c^4}{E(1+z)}}^{\infty} \frac{\bar{\varphi}\left[\frac{\epsilon E(1+z)}{m^2c^4}\right] d\epsilon}{[(\epsilon-\epsilon_i)^2 + (\omega_i/2)^2]\epsilon^2}\right)$$

where $\bar{\varphi}$ is defined in [7, 5]. Here $n_i \simeq 1.66\times10^{11}\left(\frac{L_{i,45}}{\epsilon_{i,eV} R^2_{BLR,17}} cm^{-3}\right)$, with $L_1 = L_{BLR}/(1+f)$ for Lyα photons and $L_2 = f\ L_{BLR}/(1+f)$ for OIV+Lyβ photons, where $f = 0.18$.

The integrated opacity we obtain is $\tau_{\gamma\gamma}(E,z) = R_{BLR} \times \frac{d\tau_{\gamma\gamma}}{dx}(E,z)$.

[1] http://fermi.gsfc.nasa.gov/ssc/data/analysis/

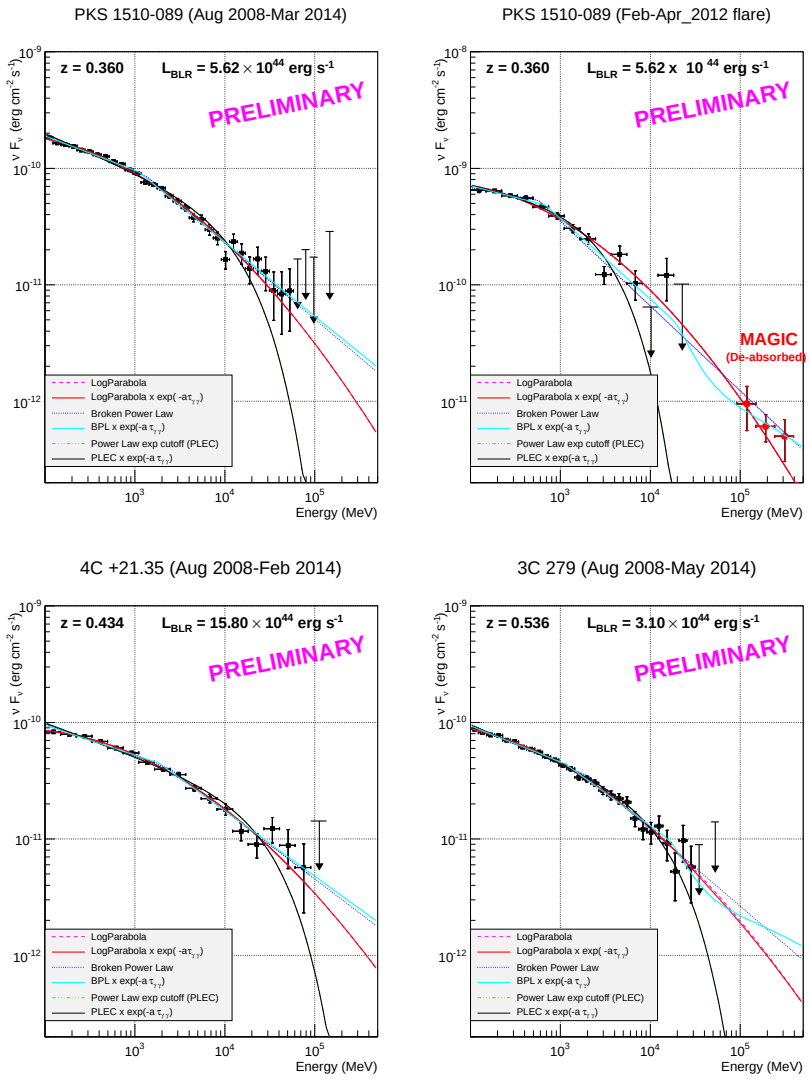

Figure 1. νF_ν SEDs of PKS 1510-089 (all 5.5 yr of data and flare), PKS 1222+216 (4C +21.35) and 3C 279. *PLEC* and *LP* fits are hidden beneath $PLEC\tau$ and $BPL\tau$.

4. Preliminary results and discussion

We produced the SEDs of the 7 bright sources we presented earlier between 100 MeV up to a few tens of GeV. In figure 1 are presented the three TeV sources PKS 1510-089, 4C +21.35 (also called PKS 1222+216), and 3C 279. PKS 1510-089 is also presented during its Feb-Apr 2012 flare, when data were taken by the MAGIC gamma-ray telescope. In figure 2 (top) is presented 3C 454.3, during three different periods that represent three different states: the first two years of data (Aug 2008-Aug 2010), the giant flare of Autumn 2010, the last three years of data (till January 2014). Before the giant flare, 3C 454.3 was often in a high activity state, whereas after December 2010, flaring episodes were rare and did not last for a long period. In figure 2 (bottom) are presented three additional sources, each one at a redshift $z \geq 0.9$: 4C +55.17, PKS 054-234 and PKS 1502+106. The LAT data points are not corrected for the absorption of extragalactic background radiation (*i.e.* not deabsorbed).

Most of the FSRQ SEDs are usually well fitted using at least one of the three following

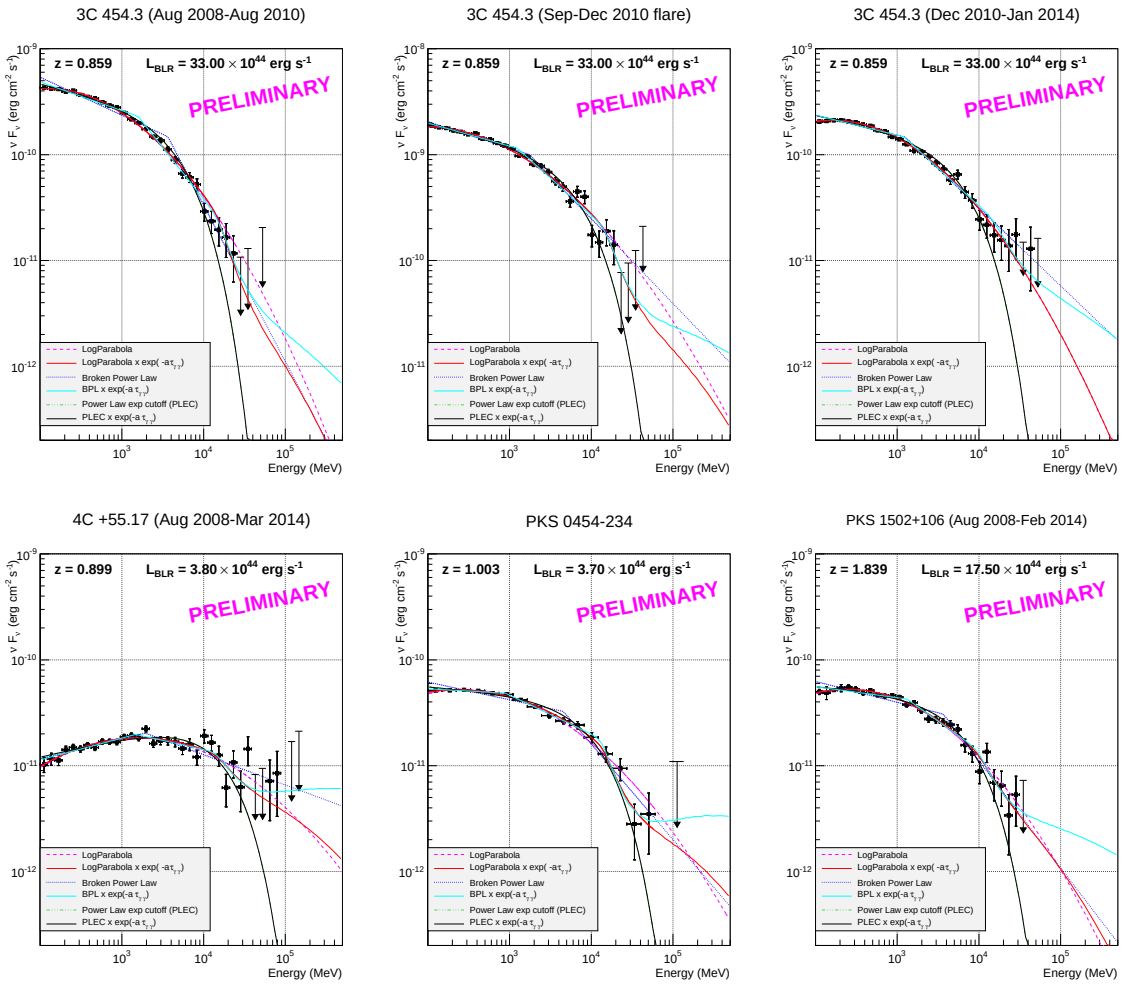

Figure 2. νF_ν SEDs of 3C 454.3 during three observation periods and for the three higher redshift sources. $PLEC$ and LP fits might be hidden beneath $PLEC\tau$ and $BPL\tau$.

functions in the MeV-GeV range: a *LogParabola (LP)*, defined in this paper as $N(E) = N_0\ (E/1000\ MeV)^{-\alpha-\beta\ log(E/1000\ MeV))}$; a *broken power law (BPL)*, defined as $N(E) = N_0\ (E/E_b)^{-\Gamma_i}$, with $i = 1$ if $E < E_b$ and $i = 2$ if $E > E_b$; a *power law with an exponential cutoff (PLEC)*, defined as $N(E) = N_0\ (E/1000\ MeV)^{-\Gamma}\ exp(-E/E_c)$. We use these functions to fit the SEDs presented in this paper from 100 MeV up to the last data point preceeding an upper limit[2].

We also performed another set of three fits, by a convolution of each of the previous functions with $exp(-a\ \tau_{\gamma\gamma}(E,z))$, where a is an additional parameter that represents the fraction of the BLR in which the gamma-ray photons are traveling, assuming the hypothesis of the previous section. In this case, the observed flux would be $F_{obs}(E) = e^{-\tau_{\gamma\gamma}(E,z)} F_{int}(E)$, and these new fit functions will be refered hereafter as $LP\tau$, $BPL\tau$ and $PLEC\tau$.

We show the fit parameters of all six fits of each SED in tables 1, 2, and 3, corresponding to the plots of figure 1 and 2. When we consider the fits performed with the LP, BPL and PLEC

[2] except for the PKS 1510-089 flare SED because we added the MAGIC points, and also considered the LAT point lying between two upper limits (see Fig. 1)

Table 1. Fitting parameters and derived significances, for the three TeV sources. We indicate with (*) when a reached the lower edge of the interval for fitting.

Param	Model		PKS 1510-089	PKS 1510-089 flare	4C +21.35	3C 279
functions (no absorption)	LP	α	2.442 ± 0.010	2.450 ± 0.018	2.337 ± 0.014	2.424 ± 0.013
	LP	β	0.063 ± 0.006	0.069 ± 0.008	0.056 ± 0.010	0.055 ± 0.008
	BPL	Γ_1	2.321 ± 0.015	2.146 ± 0.050	2.278 ± 0.026	2.341 ± 0.016
	BPL	Γ_2	2.655 ± 0.041	2.728 ± 0.026	2.587 ± 0.080	2.662 ± 0.076
	BPL	E_{break}	1392 ± 226.9	570 ± 60	2465 ± 896.0	2088 ± 506.9
	PLEC	Γ	2.325 ± 0.019	2.155 ± 0.049	2.283 ± 0.032	2.311 ± 0.020
	PLEC	E_{cutoff}	16023 ± 2966.8	3324 ± 760	33678 ± 11941	16369 ± 3490.4
functions (absorption)	LP	α	2.442 ± 0.010	2.450 ± 0.018	2.337 ± 0.014	2.423 ± 0.014
	LP	β	0.063 ± 0.006	0.069 ± 0.008	0.056 ± 0.010	0.054 ± 0.009
	BPL	Γ_1	2.295 ± 0.016	2.199 ± 0.036	2.257 ± 0.028	2.309 ± 0.020
	BPL	Γ_2	2.630 ± 0.042	2.691 ± 0.076	2.560 ± 0.065	2.561 ± 0.053
	BPL	E_{break}	1092 ± 180.0	684 ± 111	1862 ± 614.8	1128 ± 274.6
	PLEC	Γ	2.325 ± 0.019	2.155 ± 0.049	2.284 ± 0.032	2.311 ± 0.020
	PLEC	E_{cutoff}	16022 ± 2967.3	3324 ± 760	33695 ± 11961	16370 ± 3491.6
a	LP		0.00001*	0.00010*	0.00001*	0.0014 ± 0.066
	BPL		0.0003 ± 0.037	0.00010*	0.00001*	0.0143 ± 0.020
	PLEC		0.00001*	0.01157 ± 0.01163	0.00001*	0.00001*
χ^2 (ndf) (no absorption)	LP		14.700 (28)	23.67 (12)	4.894 (14)	7.306 (25)
	BPL		23.265 (27)	16.75 (11)	8.759 (13)	15.286 (24)
	PLEC		42.140 (28)	51.90 (12)	15.093 (14)	13.670 (25)
χ^2 (ndf) (absorption)	LP		14.702 (27)	23.69 (11)	4.898 (13)	7.301 (24)
	BPL		16.377 (26)	13.80 (10)	8.025 (12)	11.127 (23)
	PLEC		42.144 (27)	51.90 (11)	15.098 (13)	13.671 (24)
$\Delta\chi^2$	LP		2.669e-03	0.0276	4.146e-03	5.168e-03
	BPL		6.888e+00	2.945	7.338e-01	4.159e+00
	PLEC		3.737e-03	0.000041	4.342e-03	9.954e-04
p-value	LP		9.588e-01	8.680e-01	9.487e-01	9.427e-01
	BPL		8.680e-03	8.614e-02	3.917e-01	4.141e-02
	PLEC		9.513e-01	9.949e-01	9.475e-01	9.748e-01

Table 2. Fitting parameters and derived significances for the three periods of 3C 454.3.

Param	Model		3C 454.3 (2008-2010)	3C 454.3 (Sep-Dec 2010 flare)	3C 454.3 (2010-2014)
functions (no absorption)	LP	α	2.509 ± 0.012	2.415 ± 0.012	2.412 ± 0.012
	LP	β	0.121 ± 0.006	0.086 ± 0.006	0.112 ± 0.007
	BPL	Γ_1	2.360 ± 0.013	2.249 ± 0.013	2.189 ± 0.014
	BPL	Γ_2	3.478 ± 0.093	2.801 ± 0.073	2.739 ± 0.050
	BPL	E_{break}	3650 ± 0.4	1749 ± 241	1252 ± 139
	PLEC	Γ	2.183 ± 0.019	2.184 ± 0.017	2.149 ± 0.021
	PLEC	E_{cutoff}	5144 ± 472	7221 ± 811.9	6412 ± 762
functions (absorption)	LP	α	2.501 ± 0.013	2.410 ± 0.014	2.412 ± 0.012
	LP	β	0.118 ± 0.007	0.084 ± 0.007	0.112 ± 0.007
	BPL	Γ_1	2.270 ± 0.013	2.218 ± 0.014	2.189 ± 0.014
	BPL	Γ_2	2.968 ± 0.077	2.693 ± 0.062	2.707 ± 0.058
	BPL	E_{break}	1567 ± 174	1245 ± 164	1200 ± 148
	PLEC	Γ	2.183 ± 0.019	2.184 ± 0.017	2.149 ± 0.021
	PLEC	E_{cutoff}	5143 ± 472	7222 ± 812	6412 ± 761
a	LP		0.007 ± 0.007	0.007 ± 0.012	0.00001*
	BPL		0.007 ± 0.007	0.008 ± 0.013	0.004 ± 0.005
	PLEC		0.00001*	0.00001*	0.00001*
χ^2 (ndf) (no absorption)	LP		16.598 (24)	22.034 (23)	9.693 (25)
	BPL		85.579 (23)	34.690 (22)	51.369 (24)
	PLEC		32.384 (24)	25.094 (23)	52.935 (25)
χ^2 (ndf) (absorption)	LP		15.080 (23)	21.541 (22)	9.695 (24)
	BPL		41.220 (22)	26.682 (21)	50.514 (23)
	PLEC		32.388 (23)	25.096 (22)	52.940 (24)
$\Delta\chi^2$	LP		1.518e+00	4.928e-01	2.048e-03
	BPL		4.436e+01	8.008e+00	8.547e-01
	PLEC		3.230e-03	2.377e-03	4.397e-03
p-value	LP		2.180e-01	4.827e-01	9.639e-01
	BPL		2.733e-11	4.658e-03	3.552e-01
	PLEC		9.547e-01	9.611e-01	9.471e-01

functions, the χ^2/ndf of LP is good for all the sources (~ 1). It gives better fits than BPL and PLEC, except in the case of 4C +55.17 where χ^2/ndf of BPL is similar to the LP one. Adding the extra parameter a by using the $LP\tau$, $BPL\tau$ and $PLEC\tau$ containing the opacity $\tau_{\gamma\gamma}$ allows better fits in some cases. Best fit is obtained by optimising a within a search interval between 0.00001 and 1 in our fitting programs, as a representation of the fraction of the BLR in which the γ-ray absorption may occur. In many cases, a takes the value 0.00001 ('at limit'), and in those case the corresponding fit is matching the fit without the $exp(-a\ \tau_{\gamma\gamma})$ factor (fitting line

Table 3. Fitting parameters and derived significances for the three high redshift sources.

Param	Model		4C +55.17	PKS 0454-234	PKS 1502+106
	LP	α	1.925 ± 0.016	2.233 ± 0.015	2.300 ± 0.014
	LP	β	0.087 ± 0.011	0.089 ± 0.009	0.110 ± 0.009
	BPL	Γ_1	1.810 ± 0.027	2.168 ± 0.018	2.197 ± 0.014
func	BPL	Γ_2	2.286 ± 0.049	2.903 ± 0.099	3.011 ± 0.152
(no absorption)	BPL	E_{break}	1931 ± 250	4569 ± 5	3664 ± 572
	PLEC	Γ	1.815 ± 0.024	2.063 ± 0.025	2.066 ± 0.023
	PLEC	E_{cutoff}	14831 ± 2354.0	11658 ± 2141.7	7349 ± 913.0
	LP	α	1.921 ± 0.016	2.212 ± 0.016	2.288 ± 0.017
	LP	β	0.078 ± 0.013	0.072 ± 0.011	0.101 ± 0.012
	BPL	Γ_1	1.794 ± 0.031	2.042 ± 0.023	2.104 ± 0.018
func	BPL	Γ_2	2.169 ± 0.055	2.363 ± 0.046	2.547 ± 0.074
(absorption)	BPL	E_{break}	1476 ± 245	880 ± 173	1317 ± 206
	PLEC	Γ	1.815 ± 0.024	2.064 ± 0.025	2.066 ± 0.023
	PLEC	E_{cutoff}	14833 ± 2354	11660 ± 2140	7350 ± 914
	LP		0.009 ± 0.009	0.020 ± 0.009	0.004 ± 0.003
a	BPL		0.015 ± 0.008	0.031 ± 0.009	0.007 ± 0.003
	PLEC		0.00001*	0.00001*	0.00001*
	LP		33.211 (26)	7.993 (13)	16.056 (25)
χ^2 (ndf)	BPL		31.252 (25)	35.170 (12)	69.639 (24)
(no absorption)	PLEC		42.552 (26)	16.315 (13)	32.431 (25)
	LP		32.134 (25)	3.451 (12)	14.622 (24)
χ^2 (ndf)	BPL		29.304 (24)	3.777 (11)	26.473 (23)
(absorption)	PLEC		42.554 (25)	16.317 (12)	32.440 (24)
	LP		1.078e+00	4.542e+00	1.434e+00
$\Delta\chi^2$	BPL		1.948e+00	3.139e+01	4.317e+01
	PLEC		2.342e-03	2.003e-03	9.256e-03
	LP		2.993e-01	3.307e-02	2.311e-01
p-value	BPL		1.628e-01	2.107e-08	5.030e-11
	PLEC		9.614e-01	9.643e-01	9.234e-01

superimposed on the figure and hiding the previous line). We estimate that a has large errors due to large error bars in the $>$ 10 GeV regime where the value of a become relevant in our studies. Note that fitting with the $exp(-a\ \tau_{\gamma\gamma})$ factor leads to improvements in the χ^2/ndf values in many cases. However, while comparing each LPτ, BPLτ and PLECτ model with the corresponding model (LP, BPL and PLEC respectively), and if both fits have a $\chi^2/ndf \leq 1$, we obtain a $p-value$ which indicates no possible preference to be given to the model with BLR opacity (always below 5 σ). Only the higher redshift sources PKS 0454-234 and PKS 1502+106 have a parameter a with a error bar less than half the parameter value for $BPL\tau$ and a relatively small χ^2/ndf. Though we cannot compare these $BPL\tau$ fits with their corresponding BPL fits which have a bad χ^2/ndf, we can still consider this result as showing a potential absorption that should be confirmed by more statistics. PKS 0454-234 has also good χ^2/ndf's for both LP and $LP\tau$ fit, and $a = 0.02 \pm 0.01$. We would prefer this model to the $LP\tau$ that implies a very hard spectrum beyond 50 GeV.

We are planning to study more sources and to produce more sub-data sets showing flaring activities to continue this study. 3C 454.3 is a good candidate to pursue quiescent *versus* flaring state comparison, as we were starting to do. Still we see no evidence of a strong γ-ray absorption, which indicates that the production of γ rays should not happen deep within the BLR, where the optical/UV photon flux density is higher.

Acknowledgments

The *Fermi*-LAT Collaboration acknowledges support for LAT development, operation and data analysis from NASA and DOE (United States), CEA/Irfu and IN2P3/CNRS (France), ASI and INFN (Italy), MEXT, KEK, and JAXA (Japan), and the K.A. Wallenberg Foundation, the Swedish Research Council and the National Space Board (Sweden). Science analysis support in the operations phase from INAF (Italy) and CNES (France) is also gratefully acknowledged.

References

[1] Abdo A A et al 2011 ApJ L **733**:L26
[2] Aleksic J et al 2014 A&A 569 A46

[3] Atwood W B et al 2009 ApJ **697** 1071
[4] Baldwin J A and Netzer H 1978 ApJ **226** 1-20
[5] Brown R W Mikaelian K O and Gould R J 1973 ApJ L **14** L203-L205
[6] Ghisellini G and Tavecchio F 2009 MNRAS **397** 985
[7] Gould R J and Schréder G P 1967 Physical Review **155** 5
[8] Lei M and Wang J 2014 Publications of the Astronomical Society of Japan **66** 1 id.7 (arXiv:1308.4210v1)
[9] Pacciani L et al 2014 arXiv:1312.3998v2
[10] Poutanen J and Stern B 2010 ApJ L **717**:L118
[11] Tavecchio F and Ghisellini G 2012 submitted to MNRAS (arXiv:1209.2291v1)
[12] Telfer R C Zheng W Kriss G A and Davidsen A F 2002 ApJ **565**:773-785
[13] Xiong D R and Zhang X 2014 MNRAS **441** 4 p.3375-3395